Supplemental Material for *Impacts of absorbing biomass burning aerosol on the climate of southern Africa: A Geophysical Fluid Dynamics Laboratory GCM sensitivity study.*

C. A. Randles and V. Ramaswamy

S.1 Data Sets

S.1.1 *EP*-TOMS DATA

Satellite measurements of backscattering radiances allow for the retrieval of aerosol properties on a global or near-global scale. The Ozone Monitoring Instrument (2004-present) and its predecessor the Total Ozone Mapping Spectrometer (1979-2001) provide information on aerosol optical depth and aerosol index. While the aerosol index gives a qualitative measure of aerosol absorption (usually positive (negative) for absorbing (pure scattering) aerosols), the near-UV retrieval method of *Torres et.al*. [1998; 2002; 2005] has been used to retrieve aerosol single scattering albedo (SSA) from TOMS and OMI radiances.

S.1.2 AERONET DATA

The AERONET (http://aeronet.gsfc.nasa.gov/) [*Holben et al*., 1998]) data used in the construction of the observationally-based maps in Figure 1 (a-b) includes Level 2.0, Version 2.0 daily-mean AOD from the stations listed in Table S.1. Some monthly-mean statistics, based on the AERONET climatology tables, for the AOD at each site are presented for the season August-September-October (ASO) in Table S.1. The observations of AOD from AERONET in Figure 2 are based on the AERONET climatology tables (http://aeronet.gsfc.nasa.gov/cgi-bin/climo_menu_v2_new).

S.2 Comparison of Modeled Optical Properties to Observations.

Table S.2 gives the area-weighted average BC and OC mass loading and column-integrated aerosol optical properties for the CTRL case and the four sensitivity experiments (MOZEX, HIGHEX, SSAEX, and WHITE). Recall that CTRL only has sulfate, dust, and sea salt aerosols. BC is roughly doubled between MOZEX and the other experiments (HIGHEX, SSAEX, and WHITE) while OC is multiplied by roughly a factor of 2.5. Figure S.1 shows the ASO column-load of BC and OC for the four experiments. As noted in the text, BC and OC mass distributions are scaled up below 600 hPa in HIGHEX, SSAEX, and WHITE. Figure S.2 shows the vertical distribution of BC and OC mixing ratio in all experiments. Recall that while WHITE has the same BC and OC vertical distribution as HIGHEX, its carbonaceous aerosols are treated as optically scattering. Also note that, despite differences in the vertical distribution of BC aerosol between HIGHEX and SSAEX, the gross features of the response of these two experiments to bb aerosol forcing are similar. In Figure S.2 we also show the change in atmospheric temperature and all-sky shortwave heating rate relative to the CTRL case.

Figure 2 shows a comparison of modeled monthly-mean AOD with monthly-mean climatological ground-based AERONET sun-photometer observations [*Holben et al.,* 2001] and MODIS satellite retrievals [*Kaufman et al*. 1997] at several sites in southern Africa. In the primary biomass burning region (~0-18°S; Mongu, Senanga) where observed AOD is greatest, MOZEX tends to underestimate AOD relative to the observations while the increase in OC and BC in the other sensitivity experiments serves to better capture the peak AOD during the biomass burning season (ASO). In southeastern (Inhaca and Skukuza) and eastern Africa (not shown), which are areas more removed from the primary biomass burning region, increasing OC and BC in HIGHEX, SSAEX, and WHITE causes the model to slightly overestimate the AOD compared to AERONET (however, the model AOD remains within the AERONET observed variability).

Table S.2 gives the area-averaged SSA for each experiment as well as published observations from the SAFARI-2000 field campaign. *Haywood et al*. [2003] report single scattering albedos in the

range of 0.88 to 0.91 for regional haze from *in situ* measurements in Namibia of aerosol physical-chemical properties and Mie calculations. Using nephelometer and PSAP measurements of AOD and aerosol absorption optical depth (AAOD), SSA ranged between 0.86 and 0.92 in the same regions [*Haywood et al.,* 2003]. *Formenti et al*. [2003] determined the SSA to be 0.93±0.06 at 550 nm using regression analysis of dry particle scattering and absorption coefficients against measurements of submicron aerosol mass and apparent elemental carbon. Frequency distributions of boundary-layer average ambient SSA measured aboard the UW-Convair-580 aircraft during SAFARI 2000 gave an SSA average of 0.81±0.02 for heavy smoke and 0.89±0.03 for regional background aerosol [*Magi et al.,* 2003]. *Leahy et al*. [2007] synthesized the SSA observations taken during SAFARI-2000 and AERONET data to yield a regional biomass-burning season SSA of 0.85 ± 0.02 (mean and total uncertainty). The experiments presented in this study slightly overestimate the SSA (underestimate absorption) compared to the campaign average SSA; however, the single-scattering albedos in MOZEX, HIGHEX, and SSAEX are still absorbing enough to be useful in examining the importance of bb aerosol absorption in southern Africa.

S.3 Base Case Climatology and Observations

In Figures S.3, S.4, and S.5 we compare the CTRL case surface air temperature (T_{sat}), precipitation (P) and 850-hPa winds, low-level cloud amount (LOW), column-integrated precipitable water (WVP), and sea-level pressure (SLP) to various observations and reanalysis data. These date are described below. We provide these plots for reference and comparison; it is beyond the scope of this paper to discuss discrepancies between CTRL and the observations and reanalysis. However, it must be noted that the CTRL case lacks carbonaceous (BC and OC) aerosols in this region. In Figure S.3 and S. 4 we present the average surface air temperature (T_{sat}), total precipitation, 850-hPa winds, low-cloud

amount, and column-integrated water vapor averaged for ASO for the year 2000. In Figure S.5 we show the ASO sea-level pressure and 850-hPa winds.

NASA MERRA reanalysis:

The NASA Global Modeling and Assimilation Office's (GMAO) Modern-Era Retrospective-analysis for Research and Applications (MERRA) is a reanalysis for the satellite era produced in the NASA Goddard Earth Observing System Version 5 (GEOS-5) data assimilation model (DAS) [*Rienecker et al.,* 2008]. It focuses on historical analysis of the hydrological cycle on a broad range of weather and time scales and covers the period 1979-2007 (http://gmao.gsfc.nasa.gov/research/merra). The analysis is performed at a horizontal resolution of 2/3° longitude by 1/2° latitude and 72 levels (top at 0.01 hPa). Data presented here can be obtained using the NASA GIOVANNI web-based application (http://disc.sci.gsfc.nasa.gov/giovanni).

CRU Temperature Data

The Climate Reasearch Unit (CRU) of the University of East Anglia in conjunction with Hadley Center of the UK Met Office produce a gridded monthly-mean 5° by 5° record of combined land and marine air temperature anomalies (HadCRUT3) for the period 1850-present [*Brohan et al.,* 2006; *Rayner et al.,* 2006]. These anomalies vary from the base period 1961-1990 (Absolute; [*Jones et. al,* 1999]). Data is available for download from http://www.cru.uea.ac.uk/cru/data/temperature/. Here we present the average of August, September, and October for 2000.

GPCP Monthly Rainfall

The Global Precipitation Project (GPCP) provides a global merged rainfall analysis for research and analysis (http://www.gewex.org/gpcp.html). GPCP merges data from 6,000 rain gauge stations and

satellite geostationary and low-orbit infrared passive microwave and sounding observations. These data are used to estimate monthly rainfall on a 2.5° by 2.5° global grid from 1979 to the present. Here we present the ASO average for the year 2000 of the GPCP Global Precipitation Version 2.1 Data Set [*Huffman et al.*, 2009] obtained from the NASA GIOVANNI web-based application (http://disc2.nasacom.nasa.gov/Giovanni/tovas/rain.GPCP.shtml).

ISCCP Low-level Clouds and Precipitable Water

The International Satellite Cloud Climatology Project (ISCCP) collects and analyzes radiance data from a suite of weather satellites to infer the global distribution of clouds, their properties, and their diurnal, seasonal, and inter-annual variations for the period 1983-2010 (http://isccp.giss.nasa.gov/index.html). Monthly-mean ISCCP-D2 data are available for download from http://isccp.giss.nasa.gov/products/browsed2.html. Here we present the average of August, September, and October monthly means for the year 2000 for VIS-IR low cloud amount and total column water vapor. The low-level VIS/IR cloud top is defined by the cloud top pressure and optical thickness between pressure levels 680-1000 hPa (http://isccp.giss.nasa.gov/GIFS/cloudtypes.gif). The total column water vapor represents the total precipitable water vapor in the atmosphere determined from analysis of satellite infrared sounder data and are only valid for cloud-free locations (http://isccp.giss.nasa.gov/products/variables.html).

S.5 Supplemental Material References

Brohan, P. et al. (2006), Uncertainty estimates in regional and global observed temperature changes: a new dataset from 1850, *Journal of Geophysical Research,* **111,** D12106, doi: 10.1029/2005JD006548.

Holben, B. N. et al., (1998), AERONET - A federated instrument network and data archive for aerosol characterization, *Remote Sensing of the Environment,* **66,** 1-16**.**

Huffman, G. J. et al. (2009), Improving the global precipitation record: GPCP Version 2.1, *Geophysical Research Letters,* Vol. 37, L17808, doi:10.1029/2009GL040000.

Jones, P. D. et. al. (1999), Surface air temperature and its variations over the last 150 years, *Reviews of Geophysics,* **37**, 173-199.

Rayner, N. A. et al. (2006), Improved analysis of changes and uncertainties in marine temperature measured in situ since the mid-nineteenth century: the HadSST2 dataset, *Journal of Climate,* **19**, 446-469.

Rienecker, M. et al. (2008), The GEOS-5 Data Assimilation System - Documentation of Versions 5.0.1, 5.1.0, and 5.2.0, NASA/TM-2007-104606, Vol. 27 (available as pdf at http://gmao.gsfc.nasa.gov)

Torres, O. et al. (1998), Derivation of aerosol properties from satellite measurements of backscattered ultraviolet radiation: Theoretical basis, *Journal of Geophysical Research,* **103**, 17099-17110.

Torres, O. et al. (2002), A long-term record of aerosol optical depth from TOMS observations and comparison to AERONET measurements, *Journal of the Atmospheric Science,* **59**, 398-413.

Torres, O. et. al. (2005), Total Ozone Mapping Spectrometer measurements of aerosol absorption from space: Comparison to SAFARI 2000 ground-based observations, *J. Geophys. Res.,* 110(D10S18), doi:10.1029/2004JD004611.

Station	Lat	Lon	Elevation [m]	Years	Min ASO AOD	Max ASO AOD	Total # Months in ASO	ASO Mean AOD
Ascension Island	-7	-14	30	2000-2005	0.12	0.37	15	0.23
Bethlehem	-28	28	1709	2000	0.21	0.3	3	0.24
Etosha Pan	-19	15	1131	2000	0.23	0.48	3	0.37
Illorian	8	4	350	1998-2009	0.21	0.59	28	0.34

Station	Lat	Lon	Elevation [m]	Years	Min ASO AOD	Max ASO AOD	Total # Months in ASO	ASO Mean AOD
Inhaca	-26	32	73	2000-2001	0.24	0.44	5	0.41
Kaoma	-14	24	1179	2000	0.3	1.02	2	0.66
Maun Tower	-19	23	940	2000	0.4	0.59	2	0.50
Mongu	-15	23	1107	1995-2006	0.18	0.85	35	0.51
Mwinilunga	-11	24	1430	2000	0.72	1.10	2	0.91
Ndola	-12	28	1270	2000	0.44	0.75	2	0.60
Pietersburg	-23	29	1200	2000-2006	0.22	0.4	2	0.31
Senanga	-16	23	1025	1996-2000	0.24	1.04	8	0.53
Skukuza	-24	31	150	1998-2007	0.14	0.53	30	0.31
Skukuza Aeroport	-24	31	293	2000	0.32	0.64	2	0.48
Solwezi	-12	26	1333	2000	0.62	0.95	2	0.79
Sua Pan	-20	26	900	2000	0.19	0.64	2	0.42
Swakopmund	-22	14	250	2000	0.15	0.15	1	0.15
Zambezi	-13	23	1040	1996-2000	0.35	1.08	8	0.58

Table S.1: Locations of AERONET stations over southern Africa used to construct observationally-based maps in Figure 1 (a-b). Minimum, maximum, and average monthly-mean column integrated AOD (from the AERONET climatology tables, Level 2, Version 2) at each AERONET station during the dry season (August-September-October). The number of monthly-mean observations and the period over which the observations were taken is also given.

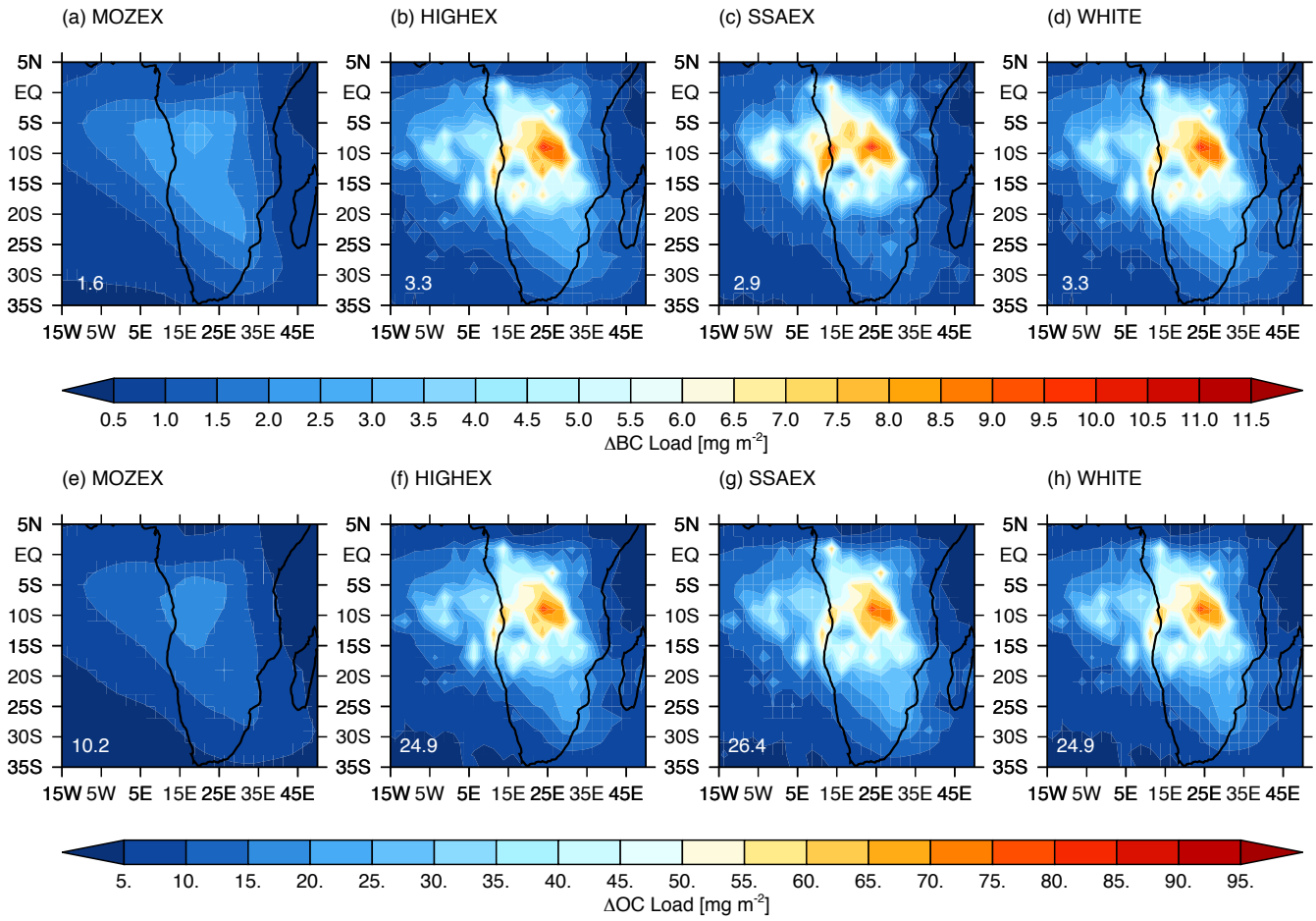

Figure S.1: ASO black carbon column load for (a) MOZEX, (b) HIGHEX, (c) SSAEX, and (d) WHITE. ASO organic carbon column load for (e) MOZEX, (f) HIGHEX, (g) SSAEX, and (h) WHITE. Note that HIGHEX and WHITE have the same BC and OC column loads, but in WHITE both BC and OC are treated optically as scattering-only aerosols. Land-area average column load is given in the bottom left of each panel.

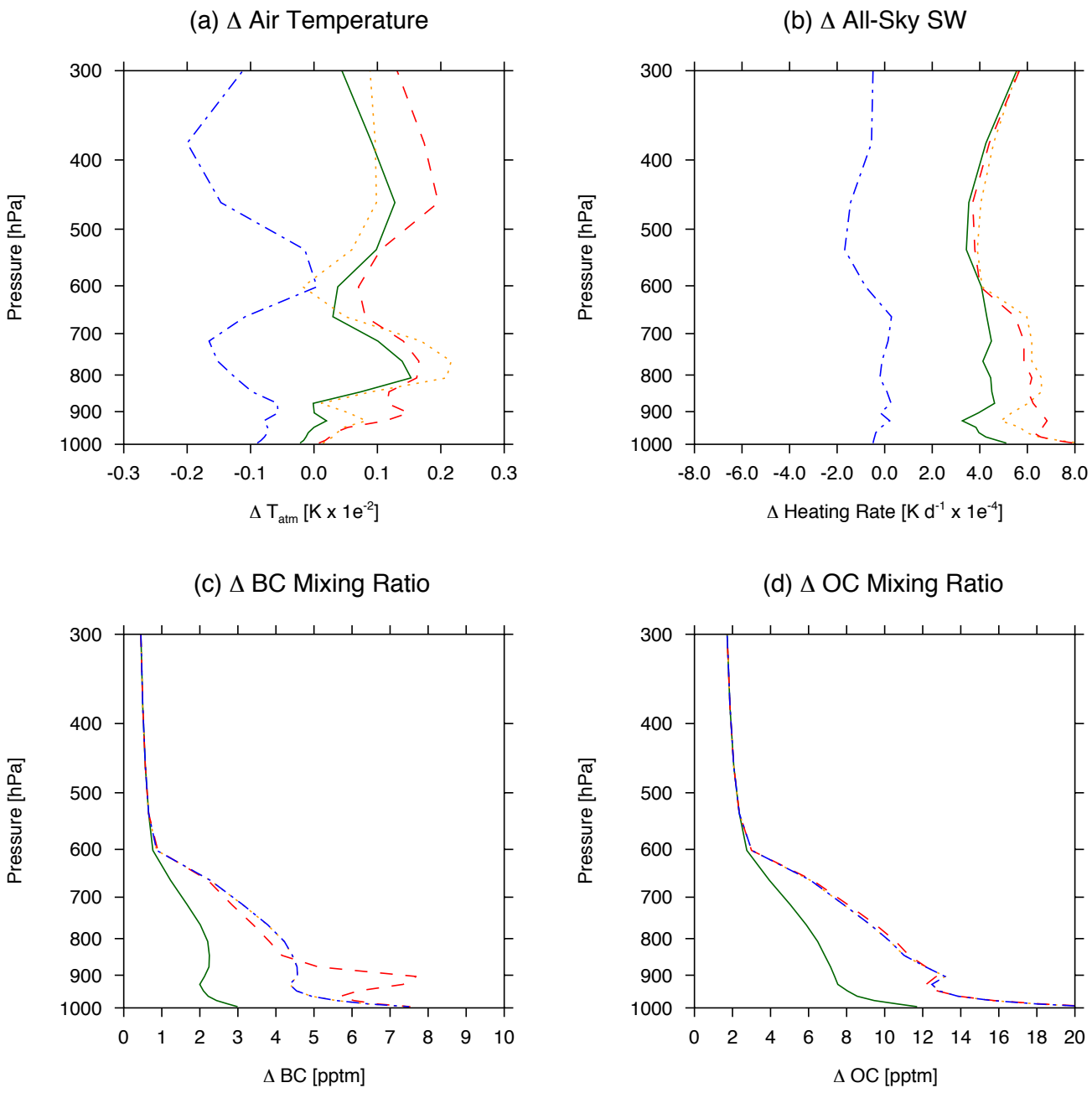

Figure S.2: ASO area-average (3°N-35°S, 0°-50°W) vertical profiles of the change in (a) atmospheric temperature (T_{atm}), (b) all-sky shortwave (SW) heating rate, (c) BC mixing ratio, and (d) OC mixing ratio relative to CTRL for MOZEX (solid green), HIGHEX (dotted orange), SSAEX (dashed red), and WHITE (dash-dotted blue). Recall OC and BC distributions are the same in HIGHEX and WHITE.

Experiment/Source	BC [Mg]	OC [Mg]	AOD	SSA
CTRL	---	---	0.10 (0.08)	0.96 (0.97)
MOZEX	19.6 (28.8)	128.0 (186.8)	0.20 (0.18)	0.90 (0.91)
HIGHEX	41.0 (56.1)	312.1 (421.4)	0.39 (0.33)	0.90 (0.91)
SSAEX	36.9 (51.2)	330.3 (447.1)	0.40 (0.34)	0.91 (0.91)
WHITE	41.0 (56.1)	312.1 (421.4)	0.38 (0.32)	0.99 (0.99)
Leahy et. al [2007]	---	---	---	0.85 ± 0.03
Haywood et. al [2003]	---	---	---	0.86 to 0.92
Magi et. al. [2003]	---	---	---	0.89 ± 0.03
Formenti et. al. [2003]	---	---	---	0.93 ± 0.06

Table S.2: ASO total mass loading of BC and OC and area-weighted average column-integrated aerosol optical properties over southern Africa (3°N-35°S, 0°-50°W). Land-only averages with land + ocean averages given in parenthesis. SAFARI-2000 observations of SSA are also presented (see text for more details); note that the *Leahy et al*. [2007] estimate represents a campaign average. Recall that CTRL only has natural aerosols (dust and sea salt) and sulfate. Differences in AOD between HIGHEX, SSAEX, and WHITE arise due to differing aerosol hygroscopic growth in each experiment, since each experiment evolves its own humidity profile; differences in SSA for MOZEX and HIGHEX are also due to aerosol hygroscopicity. The SSA in WHITE reflects absorption by natural aerosol (i.e. dust) only.

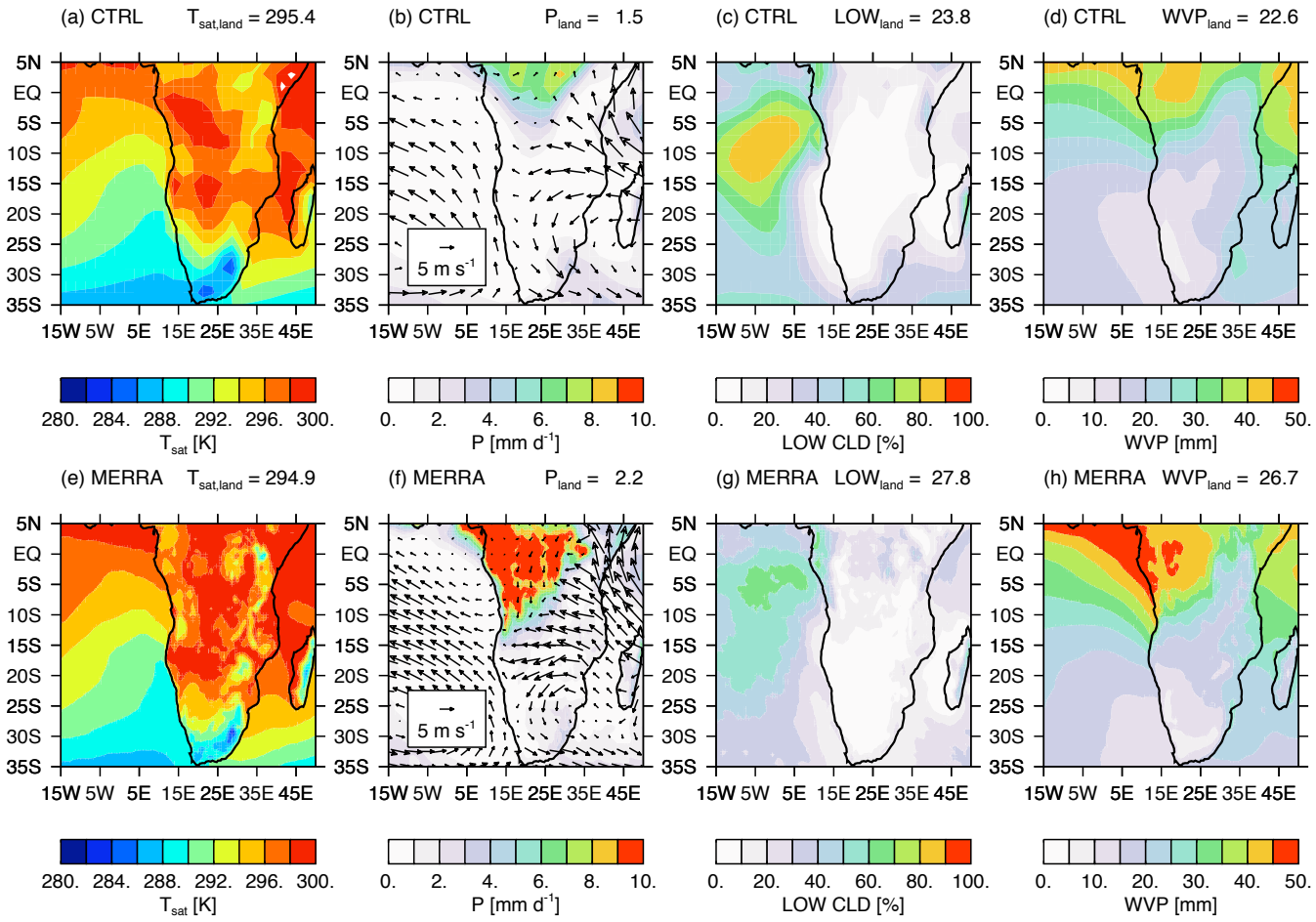

Figure S.3: ASO (a) surface air temperature (T_{sat}), (b) precipitation (P) and 850-hPa winds, low-level cloud amount (LOW), and (d) column-integrated precipitable water (WVP) for the CTRL case. ASO (e) T_{sat}, (f) P and 850-hPa winds, (g) LOW, and (h) WVP from the MERRA reanalysis for the year 2000 described in the text.

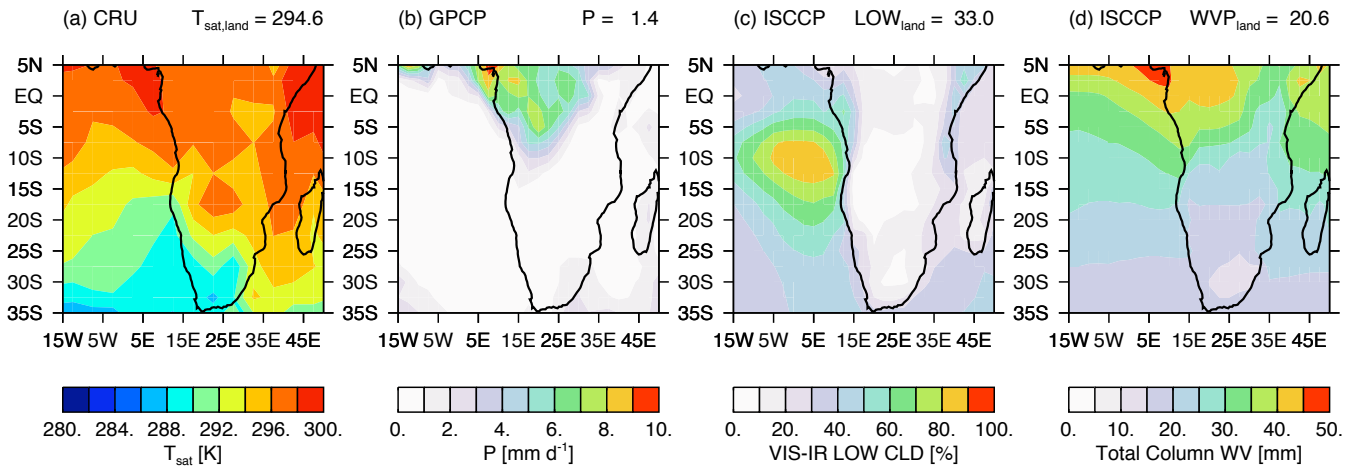

Figure S.4: Year 2000 ASO observations of (a) surface air temperature (T_{sat}) from CRU, (b) GPCP precipitation, (c) ISCCP VIS-IR low-level clouds, and ISCCP total column water vapor. See text for more details about the observational data.

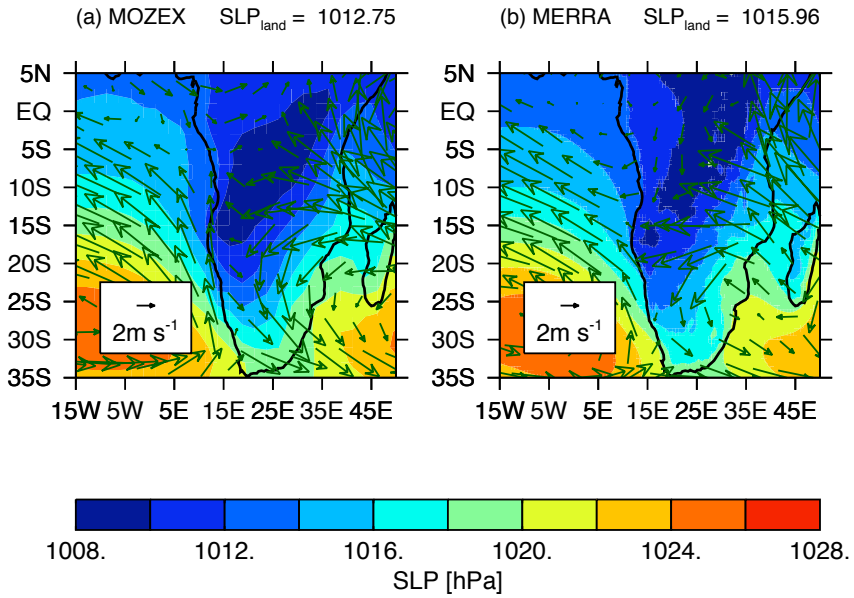

Figure S.5: (a) ASO sea-level pressure (SLP) and 850-hPa winds for the CTRL case. (b) Year 2000 MERRA reanalysis SLP and 850-hPa winds. See text for more details on the MERRA reanalysis data.